


PHYSICS

Kondo scattering in underdoped Nd_{1-x}Sr_xNiO₂ infinite-layer superconducting thin films

Ting-Na Shao ¹, Zi-Tao Zhang¹, Yu-Jie Qiao¹, Qiang Zhao¹, Hai-Wen Liu^{1,*}, Xin-Xiang Chen¹, Wei-Min Jiang¹, Chun-Li Yao¹, Xing-Yu Chen¹, Mei-Hui Chen¹, Rui-Fen Dou¹, Chang-Min Xiong¹, Guang-Ming Zhang^{2,3,*}, Yi-Feng Yang^{4,5,6,*} and Jia-Cai Nie^{1,*}

¹Department of Physics, Beijing Normal University, Beijing 100875, China;

²State Key Laboratory of Low-Dimensional Quantum Physics and Department of Physics, Tsinghua University, Beijing 100084, China;

³Frontier Science Center for Quantum Information, Beijing 100084, China;

⁴Beijing National Laboratory for Condensed Matter Physics and Institute of Physics, Chinese Academy of Sciences, Beijing 100190, China;

⁵School of Physical Sciences, University of Chinese Academy of Sciences, Beijing 100190, China and

⁶Songshan Lake Materials Laboratory, Dongguan 523808, China

*Corresponding authors. E-mails: jnie@bnu.edu.cn;

yifeng@iphy.ac.cn;

gmzhang@tsinghua.edu.cn;

haiwen.liu@bnu.edu.cn

cn

*Corresponding authors. E-mails:

jnie@bnu.edu.cn;

yifeng@iphy.ac.cn;

gmzhang@tsinghua.edu.cn;

haiwen.liu@bnu.edu.cn

cn

Received 27

September 2022;

Revised 25

December 2022;

Accepted 13 March

2023

ABSTRACT

The recent discovery of superconductivity in infinite-layer nickelates generates tremendous research endeavors, but the ground state of their parent compounds is still under debate. Here, we report experimental evidence for the dominant role of Kondo scattering in the underdoped Nd_{1-x}Sr_xNiO₂ thin films. A resistivity minimum associated with logarithmic temperature dependence in both longitudinal and Hall resistivities are observed in the underdoped Nd_{1-x}Sr_xNiO₂ samples before the superconducting transition. At lower temperatures down to 0.04 K, the resistivities become saturated, following the prediction of the Kondo model. A linear scaling behavior $\sigma_{xy}^{\text{AHE}} \sim \sigma_{xx}$ between anomalous Hall conductivity σ_{xy}^{AHE} and conductivity σ_{xx} is revealed, verifying the dominant Kondo scattering at low temperature. The effect of weak (anti-)localization is found to be secondary. Our experiments can help in clarifying the basic physics in the underdoped Nd_{1-x}Sr_xNiO₂ infinite-layer thin films.

Keywords: Kondo scattering, superconductivity, underdoped, infinite-layer nickelate, thin film

INTRODUCTION

The mechanism of high- T_c superconductivity remains a long-standing mystery, even though tremendous efforts and significant advances have been made in the study of cuprates and Fe-based superconductors. Aiming to mimic the cuprate-like electronic configuration, superconductivity has been proposed and recently found in the infinite-layer nickelate compounds [1]. This discovery has attracted great attention [2–6] as it may provide deeper insights into the pairing mechanism of unconventional superconductivity. But instead of an antiferromagnetic (AFM) order in the cuprates, the parent compound of superconducting nickelates shows no sign of static long-range magnetic order down to 1.7 K by neutron diffraction [7] and down to 2 K by muon spin measurements [8] in bulks and also a lack of long-range AFM in thin films [9], despite their similarities in the crystalline and electronic structures with the formal 3d⁹ configuration. Moreover, unlike the cuprates where doped holes re-

side on the oxygen atoms, here they are mainly introduced into Ni 3d states and reside in the 3d_{x²-y²} orbitals [10], supported by the softening of resonant inelastic X-ray scattering (RIXS) [11]. Besides, superconductivity remains absent in infinite-layer nickelate bulk, although the application of pressure up to 50.2 GPa can significantly suppress the insulating behavior [12,13]. This raises a question regarding whether the cuprates and hole doped NdNiO₂ share the same superconductivity mechanism [14]. In the experimental aspect, controlling doping concentration and studying its relationship with T_c has become a necessary step to understand the electron interaction in nickelate systems. A non-monotonic relationship between T_c and Sr doping concentration is established [3,15], reminiscent of the competition between superconductivity and adjacent phase (or its phase fluctuation) in unconventional superconductors [16–18]. It is therefore important to understand the underdoped nickelates, where, different from the cuprates, the resistivity shows

metallicity at high temperatures and weak insulating behavior at low temperatures.

In order to explain this upturn in resistivity at low temperatures, Yang and Zhang [19] proposed a self-doped Mott–Kondo scenario for the parent nickelate system, bridging the Kondo lattice model for heavy fermions and the t - J model for cuprates. It was proposed that self-doping, namely charge transfer from localized Ni 3d orbitals to other conduction bands, plays an essential role. The remaining Ni 3d local moments may couple to the conduction electrons, causing the well-known Kondo screening physics [20] and giving rise to Kondo scattering that explains the low temperature resistivity upturn reported in NdNiO₂ [1], LaNiO₂ [9], as well as underdoped infinite-layer Nd_{1-x}Sr_xNiO₂ ($x = 0.1, 0.125$) [15]. The absence of long-range magnetic ordering [9] might also be attributed to the self-doping and the Kondo screening effect. However, in addition to other theoretical scenarios including the pseudogap [21], magnetic scattering [22] and the d -wave order [23], the logarithmic temperature dependence of resistivity at low temperatures has also been observed in underdoped cuprates and was mainly attributed to weak localization (WL) [24–26]. Although it has been argued theoretically [5,27] that the transport properties of the underdoped nickelates are very different from that of the AFM cuprate Mott insulator, whether the $\ln T$ behavior in the underdoped nickelates is caused by the Kondo effect or by the WL effect has not been determined, which leads to unresolved debate concerning the basic physics of nickelate superconductors. The transport measurements, including both longitudinal and transverse resistivity, are therefore indispensable to uncover the low-energy excitations of the parent compounds of nickelate superconductor and provide conclusive evidence for different theoretical proposals in order to understand the unconventional superconductivity in the nickelate system.

Here, we study the normal-state transport properties of the infinite-layer Nd_{1-x}Sr_xNiO₂ thin films with a low Sr doping concentration. Our preliminary analysis of the film reveals a $\ln T$ behavior in both resistivity and R_H in the same temperature region. At lower temperatures down to 0.04 K, the resistivity becomes saturated. Good agreement between the experimental data and the theoretical prediction of the Kondo scenario provides conclusive evidence for the Kondo mechanism. Moreover, a linear dependence of the anomalous Hall-effect (AHE) conductance $\sigma_{xy}^{AHE} \sim \sigma_{xx}$ indicates that Kondo scattering plays a dominant role in the corresponding temperature range. The electron dephasing rate deduced from the magnetoresistance data shows a linear temperature dependence below the Kondo

temperature (T_K), in good agreement with the Kondo scenario. Last, careful analysis demonstrates that the effect of weak (anti-)localization plays only a secondary role. Our experimental results strongly support the self-doped Mott–Kondo scenario for the underdoped Nd_{1-x}Sr_xNiO₂ infinite-layer superconducting thin films.

RESULTS

Figure 1a shows the temperature-dependent resistivity $\rho(T)$ for the underdoped Nd_{0.88}Sr_{0.12}NiO₂ thin film. A superconducting transition is observed, with an onset at 4.06 K and a midpoint at 0.79 K. The broad transition indicates the inhomogeneity of the infinite-layer thin film. These observations reveal that the infinite-layer nickelate phase (the structural characterizations are shown in Supplementary Figs S1–S2), not the reduced secondary phase, is superconducting. As shown in Fig. 1a, the resistivity of the Nd_{0.88}Sr_{0.12}NiO₂ thin film first decreases as the temperature decreases, followed by a resistivity minimum at a characteristic temperature $T^* \sim 40$ K. The minimum resistivity (~ 0.80 m Ω ·cm at 40 K) falls below the value of 0.87 m Ω ·cm that corresponds to the quantum sheet resistance ($h/e^2 \sim 26$ k Ω) per NiO₂ two-dimensional plane, which is consistent with the previous report [15]. Below 30 K down to 7 K, the resistivity shows logarithmic temperature dependence regardless of the magnetic field (see Fig. 1b). In fact, this characteristic is commonly observed in all our underdoped Nd_{1-x}Sr_xNiO₂ infinite-layer thin films, as shown in Fig. 1c. We find that the ρ - T curves can be well described by the Hamann model from 8 K to 120 K [28],

$$\rho(T) = \rho_0 + aT^2 + bT^5 + \rho_K(T/T_K), \quad (1)$$

where T_K is the Kondo temperature, ρ_0 is the residual resistivity caused by sample disorder and the T^2 and T^5 terms are the contributions of electron-electron and phonon-electron interactions, respectively. $\rho_K(T/T_K)$ is the resistivity induced by magnetic scattering in the absence of magnetic field [28,29] and takes the form,

$$\rho_K(T/T_K) = \frac{2\pi c\hbar}{ne^2k_F} \left\{ 1 - \ln(T/T_K) \cdot [\ln^2(T/T_K) + s(s+1)\pi^2]^{-1/2} \right\}, \quad (2)$$

where $k_F = 2\pi(\frac{3n}{8\pi})^{1/3}$ is the Fermi wave-vector in a free electron approximation. The best fitting results to the ρ - T curves of underdoped Nd_{1-x}Sr_xNiO₂

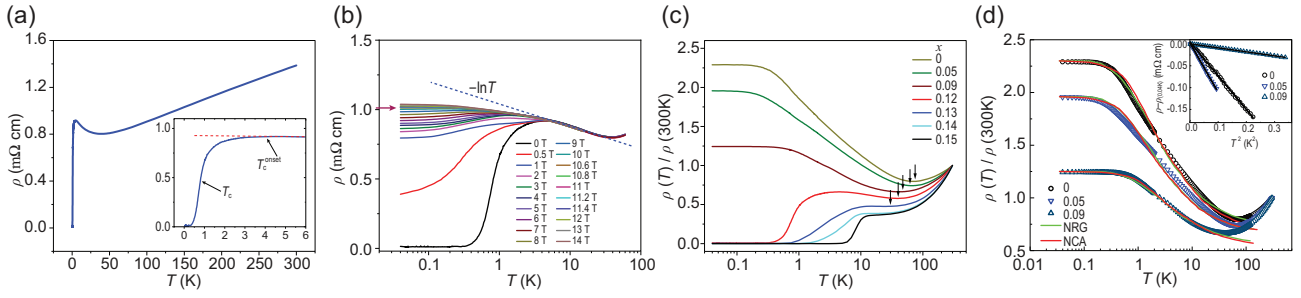


Figure 1. Temperature-dependent resistivity $\rho(T)$ for the underdoped $\text{Nd}_{1-x}\text{Sr}_x\text{NiO}_2$ thin films. (a) The temperature-dependent resistivity of the $\text{Nd}_{0.88}\text{Sr}_{0.12}\text{NiO}_2$ film at zero magnetic field. T_c and T_c^{onset} , marked by black arrows, are 0.79 K and 4.06 K, respectively. The inset shows the determination of T_c^{onset} . (b) Isomagnetic $\rho(T)$ curves of the $\text{Nd}_{0.88}\text{Sr}_{0.12}\text{NiO}_2$ film measured in different applied magnetic field H . (c) The zero-field temperature dependence of resistivity of the underdoped $\text{Nd}_{1-x}\text{Sr}_x\text{NiO}_2$ films with a Sr doping level x from 0.00 to 0.15. The arrows indicate the corresponding resistivity minima. (d) The NRG (green) and NCA (red) fits are shown for the underdoped samples with $x = 0, 0.05$ and 0.09 , and $T_K = 3.5$ K, 3.5 K and 5.5 K, respectively (see details in Fig. S4). Inset in (d) shows T^2 behavior at the lowest temperatures for the underdoped samples. See online supplementary material for a colour version of this figure.

samples using Eqs. (1) and (2) are shown in Supplementary Fig. S5. Moreover, we have carried out low-temperature transport measurements in the magnetic field for three underdoped $\text{Nd}_{1-x}\text{Sr}_x\text{NiO}_2$ samples ($x = 0, 0.05, 0.09$). All three underdoped samples are well consistent with the Kondo scattering scenario [20] down to 0.04 K. The numerical renormalization group (NRG) fitting, non-crossing approximation (NCA) fitting (see Fig. 1d and Supplementary Fig. S4) and Hamann fitting (Supplementary Fig. S5) curves provide quantitative justification for this point. The magnetic field truly influences the R - T curves of underdoped samples with pronounced negative magnetoresistance (as shown in Supplementary Fig. S5), reminiscent of the well-known negative magnetoresistance in the Kondo system $(\text{La}, \text{Ce})\text{Al}_2$ [30]. Moreover, all the underdoped samples (Fig. 1d) demonstrate clear features of Kondo scattering in temperature regime above T_K . For temperatures below ~ 0.6 K, the resistivity of the underdoped samples clearly follows a T^2 temperature dependence (inset of Fig. 1d), as expected for Kondo-like behavior [31,32]. The good agreement with the NRG, NCA and Hamann predictions proves exclusively the Kondo mechanism and leaves little room for alternative interpretation in the underdoped region, which also confirms that the local moment is roughly spin-1/2. This excludes its possible origin from the Nd 4f spin ($S = 3/2$) and supports its origin from the Ni $3d_{x^2-y^2}$ moment.

DISCUSSION

Remarkably, for temperatures below 40 K down to 6 K, the R_H follows closely that of the resistivity ρ , and resembles the $\ln T$ dependence of the resistivity, as shown in Fig. 2a (please note the sign, when the temperature decreases in the regime below 40 K,

$|R_H|$ increases rather than decreases). The $R_H \propto \rho$ behavior is well consistent with the theoretical prediction of Kondo skew scattering associated with local moments [33,34]. Thus, both the resistivity and Hall coefficient support the presence of magnetic Kondo scattering in the underdoped nickelate superconductor. The relation between σ_{xy}^{AHE} and σ_{xx} can further confirm the skew scattering mechanism characterized by $\sigma_{xy}^{\text{AHE}} \propto \sigma_{xx}$ in a temperature range of 7–40 K for the $\text{Nd}_{0.88}\text{Sr}_{0.12}\text{NiO}_2$ thin film (see Fig. 2b). The conductivity σ_{xx} of the $\text{Nd}_{0.88}\text{Sr}_{0.12}\text{NiO}_2$ is about $10^3 \Omega^{-1} \text{cm}^{-1}$ and is in a bad metal regime [34], in which σ_{xy}^{AHE} should generally decrease with decreasing σ_{xx} at a rate faster than linear. Nevertheless, by subtracting the ordinary Hall effect (OHE) contribution (R_0 , which is determined by the measured Hall coefficients and the Curie–Weiss fit and does not change with varying temperature, see detailed discussion in Eqs. (4) and (5) and results in Fig. 3a) to obtain σ_{xy}^{AHE} from σ_{xy} , a linear dependence of $\sigma_{xy}^{\text{AHE}} \propto \sigma_{xx}$ is observed in the temperature range of 7–40 K. This temperature range is the same as the range where resistivity shows logarithmic temperature dependence (see Fig. 2a). These observations strongly support that the incoherent skew scattering [33,34] is a dominant mechanism for understanding our $R_H(T)$ results. At high temperatures (> 40 K), the Kondo scattering is suppressed and a deviation from the linear dependence between σ_{xy}^{AHE} and σ_{xx} is also observed.

One may argue that the logarithmic temperature dependence of resistivity at low temperatures, a hallmark of the Kondo effect, could also originate from the weak localization/weak anti-localization (WL/WAL) in a two-dimensional system. However, as shown in Fig. 1b, the $\ln T$ correction of resistivity under a large magnetic field can exclude the WL/WAL correction and justify the Kondo scat-

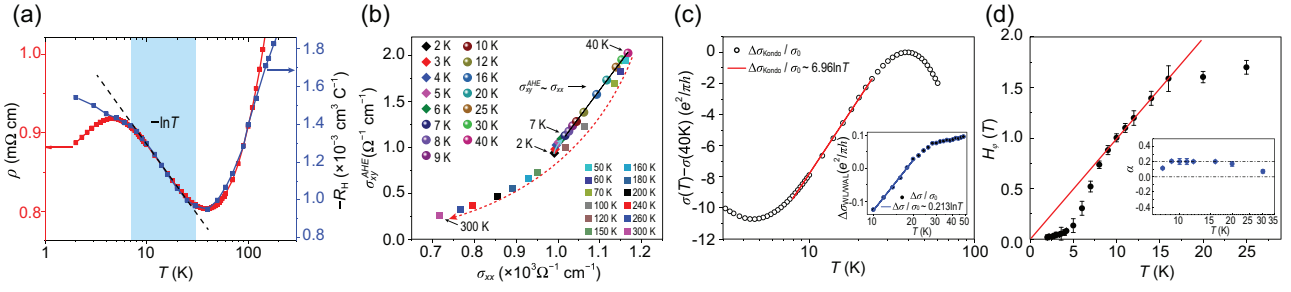


Figure 2. Scaling behavior of anomalous Hall conductivity and conductance corrections for $\text{Nd}_{0.88}\text{Sr}_{0.12}\text{NiO}_2$. (a) Logarithmic temperature dependence of the resistivity (red) and the Hall coefficient (blue) of the $\text{Nd}_{0.88}\text{Sr}_{0.12}\text{NiO}_2$ film. The light cyan area represents the Kondo region. (b) Plot of AHE conductivity σ_{xy}^{AHE} vs conductivity σ_{xx} of the $\text{Nd}_{0.88}\text{Sr}_{0.12}\text{NiO}_2$ film over the entire temperature range. Since $\rho_{xy} \sim \rho_{xx}/10^3$, we can simplify the anomalous Hall conductivity as $\sigma_{xy}^{\text{AHE}} = -\rho_{xy}^{\text{AHE}}/\rho_{xx}^2$, here $\rho_{xy}^{\text{AHE}} \equiv (\rho_H - R_0) \cdot H$, and the longitudinal conductivity as $\sigma_{xx} = 1/\rho_{xx}$. A linear dependence (solid black line) of $\sigma_{xy}^{\text{AHE}} \sim \sigma_{xx}$ is obvious in a temperature range of 7–40 K. (c) Zero field conductance correction for the $\text{Nd}_{0.88}\text{Sr}_{0.12}\text{NiO}_2$ film due to the Kondo effect, i.e. $\Delta\sigma_{\text{Kondo}} = \sigma(T) - \sigma(T_{\min} = 40\text{K})$. Data are extracted from Fig. 1b and the solid red line is the $\ln T$ fits. Inset: Conduction correction due to the WL/WAL effect, which is obtained with $\Delta\sigma_{\text{WL/WAL}} = \sigma(T)|_{H=0} - \sigma(T)|_{H=4\text{T}}$ (solid circles). The solid blue line is the $\ln T$ fit for obtaining $\Delta\kappa = \alpha p$, and here $\sigma_0 = e^2/\pi h$. (d) Dephasing field H_ϕ versus temperature for the $\text{Nd}_{0.88}\text{Sr}_{0.12}\text{NiO}_2$ film. The straight red line is the linear fit. The inset shows the corresponding α values, which are nearly constant in the temperature range of 9–20 K. See online supplementary material for a colour version of this figure.

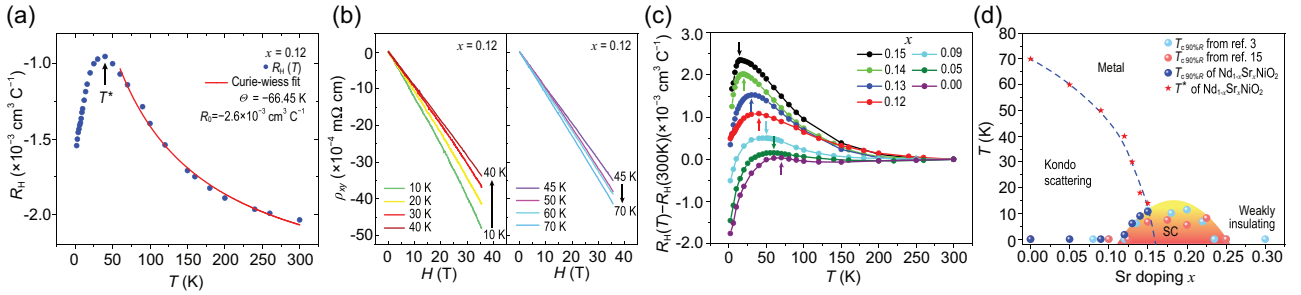


Figure 3. Kondo scattering dominated region in phase diagram of $\text{Nd}_{1-x}\text{Sr}_x\text{NiO}_2$. (a) Hall coefficient $R_H(T)$ acquired in a field of 9 T for the $\text{Nd}_{0.88}\text{Sr}_{0.12}\text{NiO}_2$ film with a maximum around 40 K. (b) Measured Hall resistivity, ρ_{xy} , versus magnetic field, H , at different temperatures. The Hall resistivity ρ_{xy} shows no obvious deviation from linear dependence on magnetic field H up to 35 T at all temperatures. (c) Hall coefficient $R_H(T) - R_H(300\text{K})$ acquired in a field of 9 T for the underdoped $\text{Nd}_{1-x}\text{Sr}_x\text{NiO}_2$ films, with a maximum around T^* , at which the resistivity normally shows a minimum (see the arrows in Fig. 1c). The corresponding characteristic temperatures T^* are indicated by the arrows. (d) The superconducting transition temperature T_c (circles) and the characteristic temperature T^* (stars) where the R_H shows a maximum (Fig. 3c). The $T_{c90\%R}$ is defined to be the temperature at which the resistivity drops to 90% of the value at the onset of the superconductivity. The cyan and orange circles represent the average $T_{c90\%R}$ adapted from references [3,15]. The blue circles represent the $T_{c90\%R}$ of the samples shown in this study.

tering scenario. The conductance correction due to the Kondo effect can be obtained with $\Delta\sigma_{\text{Kondo}} = \sigma(T) - \sigma(T_{\min} = 40\text{K})$ (zero field) and the data (extracted from Fig. 1b) are shown in Fig. 3a. The red line is the $e^2/\pi h \cdot \ln T$ fit for $\Delta\sigma$, the obtained slope is $\beta \approx 6.96$ for the temperature range of 8–24 K. Although both the WL/WAL and the electron-electron interaction (EEI) in a two-dimensional system also contributes to a conductance correction proportional to $e^2/\pi h \cdot \ln T$, the total value for the coefficient of WL/WAL and EEI corrections is commonly less than 2 [35]. Thus, the value of β is much larger than the typical value contributed from WL/WAL and EEI effect (see Supplementary Note 1). In order to single out the WL/WAL correction,

the measurement in a modest magnetic field (e.g. $H = 4\text{T}$) is necessary (Supplementary Fig. S8). The conduction correction due to the WL/WAL effect can be obtained with $\Delta\sigma_{\text{WL/WAL}} = \sigma(T)|_{H=0} - \sigma(T)|_{H=4\text{T}}$, and the data are shown in the inset of Fig. 2c. The blue line is the $\ln T$ fit, the obtained slope is $\Delta\kappa = \alpha p \approx 0.213$ (p is the dephasing exponent and denotes the strength of dephasing rate versus temperature, $\tau_\phi^{-1} \sim T^p$ [35]) for the temperature range of 10–20 K, much less than the total value $\beta \approx 6.96$, indicating that the WL/WAL is a secondary effect and Kondo scattering is dominant in the temperature range of 7–30 K. See online supplementary material for a colour version of this figure.

Moreover, we can also utilize the low field magneto-conductivity to analyze the temperature dependence of electron dephasing, based on the modified Hikami–Larkin–Nagaoka (HLN) formula [36]:

$$\Delta\sigma(H) = \frac{\alpha e^2}{\pi h} \left[\Psi \left(\frac{1}{2} + \frac{H_\varphi}{H} \right) - \ln \frac{H_\varphi}{H} \right], \quad (3)$$

where Ψ is the digamma function, $H_\varphi = \hbar/4eD\tau_\varphi$, D is the electronic diffusion constant, and α is an effective constant depending on the relative strengths of magnetic scattering and spin-orbit coupling (see Supplementary Figs S8–S9 for related results and see Supplementary Figs S10–S14 for detailed analysis). As shown in the inset of Fig. 2d, for the nickelate thin film studied this work, a small positive value $\alpha \approx 0.20$ can be maintained for a wide temperature range of 9–20 K. As the dephasing rate τ_φ^{-1} is simply proportional to H_φ , there exists a linear power-law dependence: $H_\varphi \sim T^p$ with $p \approx 1$. Indeed, as shown in Fig. 2d, a linear temperature dependence of the dephasing field H_φ is observed over a wide temperature range of 8–16 K below T_K , which is consistent with the universal dephasing rate due to Kondo impurities [37]. At temperatures below 8 K, the deviation of $\tau_\varphi^{-1} \propto T$ might originate from the influence of superconductivity fluctuation. The dephasing field H_φ also exhibits a deviation from the linearity around ~ 16.0 K. This is due to resonant Kondo scattering in the vicinity of the Kondo temperature and is another definition of T_K [38,39]. The obtained value of T_K (~ 16.0 K) is well consistent with that (~ 15.6 K, see Supplementary Fig. S5d) determined by the resistivity measurements. Thus, the Kondo scenario provides a consistent explanation of all our measured data.

Figure 3a displays the Hall-effect measurements obtained in large temperature range under an applied field of 9 T, showing negative Hall coefficients (R_H) with a maximum at $T^* \sim 40$ K. Interestingly, we find the Hall coefficients now follow a simple Curie–Weiss law. To see this, we separate the normal coefficient R_0 from the AHE coefficient and make the ansatz based on the treatment of heavy fermion superconductors [40]

$$\rho_{xy} = R_0 H + 4\pi M R_S. \quad (4)$$

Taking $M = \chi H$, $\chi = C/(T - \Theta)$, where M is the magnetization, χ is the magnetic susceptibility, C is the Curie constant and Θ is the Curie temperature, we have

$$R_H = \frac{\rho_{xy}}{H} = R_0 + 4\pi \frac{C}{T - \Theta} R_S = R_0 + \frac{R'_S}{T - \Theta}, \quad (5)$$

with three fitting parameters. R_0 is the OHE coefficient due to deflection of the conduction electrons by the Lorentz force. We obtain a good fit which satisfies the Curie–Weiss law for $60 \text{ K} \leq T \leq 300 \text{ K}$. The best fit (solid line in Fig. 3a) was obtained at $R_0 = -2.61 \times 10^{-3} \text{ cm}^3 \text{ C}^{-1}$, $\Theta = -66.45 \text{ K}$ and $R'_S = 0.20 \text{ cm}^3 \text{ KC}^{-1}$. R_0 was found to be negative, which means that the OHE is dominated by electrons. This is consistent with the band structure calculations revealing that the parent NdNiO_2 contains small electron pockets at the Fermi energy [41], which is valid even for the underdoped samples of the same doping level based on the published Hall data [3,15]. At high temperatures ($> 50 \text{ K}$), the Kondo scattering is suppressed and the AHE contribution decreases with increasing temperature, resulting in an increase in $|R_H|$ accordingly (Fig. 2a). The fitting value R_0 corresponds to 0.12 electron per formula unit. As shown in Fig. 3b, the Hall resistivity ρ_{xy} versus magnetic field up to 35 T at temperatures from 10 K to 70 K shows no obvious deviation from linear dependence on the magnetic field (also see Supplementary Fig. S7 for the extended temperature region data). Such Curie–Weiss type temperature dependence of the positive AHE coefficient is repeatedly observed in our underdoped $\text{Nd}_{1-x}\text{Sr}_x\text{NiO}_2$ infinite-layer thin films (as shown in Fig. 3c) and is also common in recently reported nickelate superconductors [3,14,15,42]. It supports the existence of free local moments at high temperatures where the Kondo scattering is negligible, and the resistivity is dominated by electron-phonon scattering. The negative values of the Weiss temperature Θ indicate AFM correlations in the localized-spin systems. Actually, a magnetic ground state is often obtained in theoretical studies [6,10,39,43,44]. A branch dispersion of magnetic excitations in undoped NdNiO_2 has recently been revealed using RIXS [45], suggesting a spin wave of strongly coupled, antiferromagnetically aligned spins on a square lattice. A recent NMR study shows the presence of AFM fluctuations and quasi-static AFM order in $\text{Nd}_{0.85}\text{Sr}_{0.15}\text{NiO}_2$ [46] thin film. However, the tendency toward a long-range AFM order is interrupted by the self-doping and Kondo screening effect, causing a paramagnetic state (see the positive χ , i.e. the positive AHE coefficient in Fig. 3a) as reported so far for all RNiO_2 ($R = \text{rare-earth}$) parent materials [7,9]. Most recently, charge density wave states were repeatedly discovered in the parent and underdoped nickelates [47–49], which suggest a great level of similarity to cuprates. It was remarked that a charge order modulation would also disfavor the formation of long-range AFM order. In other words, the competition between the charge order and the AFM correlation might be another reason why

long-range AFM order has not been observed. In a recent theoretical work, it has also been proposed that the charge order might be associated with electron transfer from Ni 3d orbitals to conduction bands close to the Fermi energy and thus provide a condition for the presence of Kondo scattering at low temperatures [50].

Based on the present findings, Fig. 3d depicts a phase diagram of the $\text{Nd}_{1-x}\text{Sr}_x\text{NiO}_2$ showing a superconducting dome, combined with that in recent reports [3,15,51,52], and the characteristic temperature T^* , where the R_H shows a maximum. As x increases from the underdoped side, T^* decreases monotonically and the T^*-x curve separates the underdoped region into two parts: a Kondo scattering region and a metal. It is worth noting that the extension of the T^*-x curve reaches the bottom of the superconducting dome (under magnetic field), which is well consistent with the recent report [52]. Thus, instead of a simple Mott insulator, the Kondo physics must also play a crucial role in nickelate superconductors. Our results may indeed have some implications on the superconductivity. Based on the Kondo mechanism in the underdoped region, our phase diagram (see Fig. 3d) suggests that superconductivity emerges near the boundary and that the Kondo effect is suppressed. As discussed previously [19], this may have an important influence on the pairing symmetry of the superconductivity. The interplay of magnetic fluctuations and Kondo hybridization could potentially lead to $d + is$ pairing [19].

CONCLUSION

Putting everything together, the logarithmic temperature dependence of resistivity and R_H , the good agreement with the NRG, NCA and Hamann predictions, the linear dependence of $\sigma_{xy}^{\text{AHE}} \sim \sigma_{xx}$, and the linear temperature dependence of the dephasing rate, all support the presence of magnetic Kondo scattering in the underdoped infinite-layer $\text{Nd}_{1-x}\text{Sr}_x\text{NiO}_2$ thin film. According to Yang and Zhang [19], the presence of local moments cannot be ascribed to the Nd 4f moments since similar transport properties have also been observed in LaNiO_2 [9]. The first-principles band structure calculations [41] show that the Nd 5d orbitals in NdNiO_2 are hybridized with the Ni 3d orbitals, leading to small Fermi pockets of dominantly Nd 5d electrons in the Brillouin zone. Nd 5d conduction electrons have an electron density of $n < 1$ per Ni site, coupled to the localized Ni^{1+} spin-1/2 of $3d_{x^2-y^2}$ orbital to form Kondo spin singlets, as in the Kondo lattice systems with a small concentration of conduction electrons [20]. In conclusion, our experimental re-

sults strongly support the self-doped Mott-Kondo scenario for the underdoped $\text{Nd}_{1-x}\text{Sr}_x\text{NiO}_2$ infinite-layer thin films. The present findings shed new light on the underlying physics of the infinite-layer nickelates and a possibly novel mechanism of unconventional superconductivity. It would improve our understanding of the newly discovered superconductivity in nickelates.

SUPPLEMENTARY DATA

Supplementary data are available at [NSR](https://doi.org/10.1093/nsr/nwad112) online.

ACKNOWLEDGEMENTS

The authors thank Prof. Mingliang Tian, from High Magnetic Field Laboratory of Chinese Academy of Sciences at Hefei, for his support to the high magnetic field measurements.

FUNDING

This work was supported by the National Natural Science Foundation of China (92065110, 11974048, 12074334, 12174429, and 12022407), the National Basic Research Program of China (2014CB920903 and 2013CB921701), and the Strategic Priority Research Program of the Chinese Academy of Sciences (XDB33010100).

AUTHOR CONTRIBUTIONS

J.C.N. conceived the project and supervised the experiments. T.N.S. and Y.J.Q. grew the nickelate films and conducted the reduction experiments and structural characterization. T.N.S., Z.T.Z. and Q.Z. performed the transport measurements and analysis with X.X.C., W.M.J., C.L.Y., X.Y.C., M.H.C., C.M.X., and R.F.D. J.C.N., T.N.S. and H.W.L. wrote the manuscript with help from G.M.Z., Y.F.Y. and with input from all authors.

Conflict of interest statement. None declared.

REFERENCES

- Li D, Lee K and Wang BY *et al.* Superconductivity in an infinite-layer nickelate. *Nature* 2019; **572**: 624–7.
- Gu Q, Li Y and Wan S *et al.* Single particle tunneling spectrum of superconducting $\text{NiNd}_{1-x}\text{Sr}_x\text{NiO}_2$ thin films. *Nat Commun* 2020; **11**: 6027.
- Zeng S, Tang CS and Yin X *et al.* Phase diagram and superconducting dome of infinite-layer $\text{Nd}_{1-x}\text{Sr}_x\text{NiO}_2$ thin films. *Phys Rev Lett* 2020; **125**: 147003–7.
- Goode BH, Li D and Lee K *et al.* Doping evolution of the Mott-Hubbard landscape in infinite-layer nickelates. *Proc Natl Acad Sci USA* 2021; **118**: e2007683118–7.
- Zhang Y-H and Vishwanath A. Type-II $t-J$ model in superconducting nickelate $\text{Nd}_{1-x}\text{Sr}_x\text{NiO}_2$. *Phys Rev Research* 2020; **2**: 023112–11.

6. Botana AS and Norman MR. Similarities and differences between LaNiO_2 and CaCuO_2 and implications for superconductivity. *Phys Rev X* 2020; **10**: 011024–6.
7. Hayward MA and Rosseinsky MJ. Synthesis of the infinite layer $\text{Ni}(\text{I})$ phase NdNiO_{2+x} by low temperature reduction of NdNiO_3 with sodium hydride. *Solid State Sci* 2003; **5**: 839–50.
8. Ortiz RA, Puphal P and Klett M *et al.* Magnetic correlations in infinite-layer nickelates: an experimental and theoretical multimethod study. *Phys Rev Research* 2022; **4**: 023093–19.
9. Ikeda A, Krockenberger Y and Irie H *et al.* Direct observation of infinite NiO_2 planes in LaNiO_2 films. *Appl Phys Express* 2016; **9**: 061101–3.
10. Zhang H, Jin L and Wang S *et al.* Effective Hamiltonian for nickelate oxides $\text{Nd}_{1-x}\text{Sr}_x\text{NiO}_2$. *Phys Rev Research* 2020; **2**: 013214–10.
11. Rossi M, Lu H and Nag A *et al.* Orbital and spin character of doped carriers in infinite-layer nickelates. *Phys Rev B* 2021; **104**: L220505–7.
12. Li Q, He C and Si J *et al.* Absence of Superconductivity in Bulk $\text{Nd}_{1-x}\text{Sr}_x\text{NiO}_2$. *Commun Mater* 2020; **1**: 16–8.
13. Gu Q and Wen H-H. Superconductivity in nickel-based 112 systems. *The Innovation* 2022; **3**: 100202–13.
14. Ji Y, Liu J and Li L *et al.* Superconductivity in infinite layer nickelates. *J Appl Phys* 2021; **130**: 060901–15.
15. Li D, Wang BY and Lee K. Superconducting dome in $\text{Nd}_{1-x}\text{Sr}_x\text{NiO}_2$ infinite layer films. *Phys Rev Lett* 2020; **125**: 027001–6.
16. Keimer B, Kivelson SA and Norman MR *et al.* From quantum matter to high-temperature superconductivity in copper oxides. *Nature* 2015; **518**: 179–86.
17. Hosono H. Layered iron pnictide superconductors: discovery and current status. *J Phys Soc Jpn* 2008; **77**: 1–8.
18. Dagotto E. Complexity in strongly correlated electronic systems. *Science* 2005; **309**: 257–62.
19. Zhang GM, Yang YF and Zhang FC. Self-doped Mott insulator for parent compounds of nickelate superconductor. *Phys Rev B* 2020; **101**: 020501(R)–5.
20. Hewson AC. *The Kondo Problem to Heavy Fermions* (Cambridge University Press, Cambridge, UK, 1993); Costi TA, Hewson AC and Zlatić V. Transport coefficients of the Anderson model via the numerical renormalization group. *J Phys: Condens Matter* 1994; **6**: 2519–57.
21. Laliberté F, Tabis W and Badoux S *et al.* Origin of the metal-to-insulator crossover in cuprate superconductors. arXiv:1606.04491.
22. Dagan Y, Barr MC and Fisher WM *et al.* Origin of the anomalous low temperature upturn in the resistivity of the electron-doped cuprate superconductors. *Phys Rev Lett* 2005; **94**: 057005–4.
23. Zhou X, Peets DC and Morgan B *et al.* Logarithmic upturn in low-temperature electronic transport as a signature of d -wave order in cuprate superconductors. *Phys Rev Lett* 2018; **121**: 267004–7.
24. Segawa K and Ando Y. Charge localization from local destruction of antiferromagnetic correlation in Zn-doped $\text{YBa}_2\text{Cu}_3\text{O}_{7-\delta}$. *Phys Rev B* 1999; **59**: R3948–51.
25. Fournier P, Higgins J and Balci H *et al.* Anomalous saturation of the phase coherence length in underdoped $\text{Pr}_{2-x}\text{Ce}_x\text{CuO}_4$ thin films. *Phys Rev B* 2000; **62**: R11993–6.
26. Rullier-Albenque F, Alloul H and Tourbot R. Disorder and transport in cuprates: weak localization and magnetic contributions. *Phys Rev Lett* 2001; **87**: 157001–4.
27. Hepting M, Li D and Jia CJ *et al.* Electronic structure of the parent compound of superconducting infinite-layer nickelates. *Nat Mater* 2020; **19**: 381–5.
28. Yang JY, Han YL and He L *et al.* d carrier induced intrinsic room temperature ferromagnetism in Nb:TiO_2 film. *Appl Phys Lett* 2012; **100**: 202409–4.
29. Hamann DR. New solution for exchange scattering in dilute alloys. *Phys Rev* 1967; **158**: 570–80.
30. Felsch W and Winzer K. Magnetoresistivity of (La, Ce) A_{12} alloys. *Solid State Commun* 1973; **13**: 569–73.
31. Star WM, Basters FB and Nap GM *et al.* Toward simple powers of T in the Kondo effect: I. Low-temperature electrical resistivity of dilute Cu-Fe alloys. *Physica* 1972; **58**: 585–622.
32. Matsushita Y, Bluhm H and Geballe TH *et al.* Evidence for charge Kondo effect in superconducting TI-doped PbTe . *Phys Rev Lett* 2005; **94**: 157002–4.
33. Fert A and Levy PM. Theory of the Hall effect in heavy-fermion compounds. *Phys Rev B* 1987; **36**: 1907–16.
34. Nagaosa N, Sinova J and Onoda S *et al.* Anomalous Hall effect. *Rev Mod Phys* 2010; **82**: 1539–92.
35. Lee PA and Ramakrishnan TV. Disordered electronic systems. *Rev Mod Phys* 1985; **57**: 287–337.
36. Hikami S, Larkin AI and Nagaoka Y. Spin-orbit interaction and magnetoresistance in the two-dimensional random system. *Prog Theor Phys* 1980; **63**: 707–10.
37. Micklitz T, Altland A and Costi TA *et al.* Universal dephasing rate due to diluted Kondo impurities. *Phys Rev Lett* 2006; **96**: 226601–4.
38. Peters RP, Bergmann G and Mueller RM. Kondo maximum of magnetic scattering. *Phys Rev Lett* 1987; **58**: 1964–7.
39. VanHaesendonck C, Vranken J and Bruynseraede Y. Resonant Kondo scattering of weakly localized electrons. *Phys Rev Lett* 1987; **58**: 1968–71.
40. Schoenes J and Franse JMM. Hall effect in the heavy-fermion superconductor UPt_3 . *Phys Rev B* 1986; **33**: 5138–40.
41. Karp J, Botana AS and Norman MR *et al.* Many-body electronic structure of NdNiO_2 and CaCuO_2 . *Phys Rev X* 2020; **10**: 021061–11.
42. Osada M, Wang BY and Goodge BH *et al.* Nickelate superconductivity without rare-earth magnetism: (La,Sr)NiO₂. *Adv Mater* 2021; **33**: 2104083–7.
43. Liu Z, Ren Z and Zhu W *et al.* Electronic and magnetic structure of infinite-layer NdNiO_2 : trace of antiferromagnetic metal. *npj Quantum Mater* 2020; **5**: 31–8.
44. Gu Y, Zhu S and Wang X *et al.* A substantial hybridization between correlated $\text{Ni-}d$ orbital and itinerant electrons in infinite-layer nickelates. *Commun Phys* 2020; **3**: 84–9.
45. Lu H, Rossi M and Nag A *et al.* Magnetic excitations in infinite-layer nickelates. *Science* 2021; **373**: 213–6.
46. Cui Y, Li C and Li Q. NMR evidence of antiferromagnetic spin fluctuations in $\text{Nd}_{0.85}\text{Sr}_{0.15}\text{NiO}_2$. *Chinese Phys Lett* 2021; **38**: 067401–6.
47. Tam CC, Choi J and Ding X *et al.* Charge density waves in infinite-layer NdNiO_2 nickelates. *Nat Mater* 2022; **21**: 1116–20.
48. Rossi M, Osada M and Choi J *et al.* A broken translational symmetry state in an infinite-layer nickelate. *Nat Phys* 2022; **18**: 869–73.
49. Krieger G, Martinelli L and Zeng S *et al.* Charge and spin order dichotomy in NdNiO_2 driven by the capping layer. *Phys Rev Lett* 2022; **129**: 027002–7.
50. Chen H, Yang Y-F and Zhang G-M. Charge order from the local Coulomb repulsion in undoped infinite-layer nickelates. 2022; arXiv:2204.12208.
51. Hsu Y-T, Wang BY and Berben M *et al.* Insulator-to-metal crossover near the edge of the superconducting dome in $\text{NiNd}_{1-x}\text{Sr}_x\text{NiO}_2$. *Phys Rev Research* 2021; **3**: L042015–5.
52. Lee K, Wang BY and Osada M *et al.* Character of the “normal state” of the nickelate superconductors. 2022; arXiv: 2203.02580.